DATA REPOSITORY for:

Holocene glacier culminations in the Western Alps and their hemispheric relevance

Irene Schimmelpfennig, Joerg M. Schaefer, Naki Akçar, Susan Ivy-Ochs, Robert C. Finkel, Christian Schlüchter

Geology

Table DR1: Sample details, analytical data and surface exposure ages. Sample $^{10}Be/^{9}Be$ ratios, measured at the Center for Accelerator Mass Spectrometry of the Lawrence Livermore National Laboratory, were normalized to one of the indicated standards, KNSTD (until mid-2007; $^{10}Be/^{9}Be = 3.15 \times 10^{-12}$) or KNSTD07 (after the year 2007; $^{10}Be/^{9}Be = 2.85 \times 10^{-12}$). Measurements normalized to KNSTD were corrected by a factor of 0.9048 during age calculation. The ages are calculated using the ^{10}Be production rate with a value of 3.85 ± 0.19 atoms $(g\ yr)^{-1}$ (Balco et al. 2009, normalized to standard 07KNSTD) and the scaling method 'Lm' (time-dependent version of Lal, 1991) according to Balco et al. (2008). They are reported in calendar years before 2010 CE. 1σ analytical uncertainties range between 1.5% and 3%, except for samples younger than 500 years, which have uncertainties between 3% and 10%.

Sample name	Latitude (°N)	Longitude (°E)	Elevation (m)	Thickness (cm)	Shielding factor	Qtz weight (g)	Carrier (mg ^{9}Be)	Carrier (mg ^{9}Be)	$^{10}Be/^{9}Be$ Standard used	$^{10}Be/^{9}Be$ x10^{-14}	[^{10}Be] (x 10^{3} atoms g^{-1})	^{10}Be age (years)	1σ Analyt. error	1σ error incl. prod. rate error
Pre-LIA MORAINE, BOULDERS ON CREST														
ARO-4	46.01820	7.46480	2393	2.30	0.977	9.97	0.2040	BE23706	KNSTD	25.15±0.36	332.9±4.8	11920	170	610
ARO-1	46.01824	7.46527	2387	4.36	0.977	16.55	0.2077	BE23715	KNSTD	39.93±0.66	325.1±5.4	11880	200	620
ARO-6	46.01746	7.45986	2433	2.04	0.970	21.33	0.2060	BE23716	KNSTD	54.0±1.0	338.6±6.5	11870	230	630
ARO-55	46.01838	7.46628	2371	1.89	0.977	12.04	0.1829	BE31219	07KNSTD	28.59±0.46	289.9±4.7	11610	190	600
ARO-5	46.01823	7.46434	2400	3.19	0.977	10.60	0.1991	BE23707	KNSTD	26.45±0.44	321.4±5.4	11510	200	600
ARO-52	46.01858	7.46791	2345	1.91	0.978	17.54	0.1830	BE31211	07KNSTD	40.09±0.75	279.0±5.2	11350	210	600
ARO-59	46.01752	7.4602	2432	1.43	0.970	20.08	0.1836	BE31213	07KNSTD	48.04±0.89	293.1±5.5	11290	210	600
ARO-3	46.01823	7.46509	2389	2.50	0.977	10.06	0.2043	BE23705	KNSTD	23.59±0.39	309.9±5.2	11140	190	580
ARO-56	46.01798	7.46267	2419	3.27	0.974	20.08	0.1840	BE31212	07KNSTD	45.83±0.85	279.4±5.2	10960	200	580
ARO-2	46.01824	7.46516	2389	3.31	0.977	10.07	0.2050	BE23704	KNSTD	22.85±0.38	300.9±5.1	10880	180	570
Pre-LIA MORAINE, BOULDERS ON RECESSIONAL RIDGES														
ARO-21_2010Apr	46.01762	7.46405	2393	2.13	0.943	5.57	0.1868	BE29530	07KNSTD	12.90±0.31	285.6±7.0	11650	290	640
ARO-21	46.01762	7.46405	2393	2.13	0.943	42.19	0.2053	BE24922	07KNSTD	89.6±1.8	283.1±5.7	11630	240	620
ARO-22	46.01762	7.46477	2381	2.62	0.954	5.34	0.1894	BE28931	07KNSTD	12.23±0.28	279.2±6.6	11420	270	630
ARO-21_re	46.01762	7.46405	2393	2.13	0.943	20.15	0.1839	BE31210	07KNSTD	45.49±0.85	277.0±5.2	11330	210	600
ARO-18	46.01788	7.46407	2399	1.91	0.966	4.53	0.1878	BE28930	07KNSTD	10.66±0.30	283.8±8.2	11280	330	650
ARO-8	46.01692	7.45804	2442	3.93	0.970	10.14	0.2051	BE23708	KNSTD	24.33±0.41	318.4±5.4	11230	190	590
ARO-16	46.01777	7.46387	2399	1.61	0.954	5.14	0.1860	BE28929	07KNSTD	11.92±0.21	277.7±5.1	11150	200	590
ARO-7	46.01696	7.45834	2441	2.50	0.970	30.37	0.2048	BE23717	KNSTD	72.5±1.2	317.4±5.4	11070	190	580
ARO-15	46.01773	7.46347	2404	1.63	0.954	3.66	0.1894	BE28928	07KNSTD	8.23±0.21	273.1±7.0	10910	280	610
'LIA' COMPOSITE MORAINE, OUTMOST SUB-RIDGE														
ARO-12	46.01678	7.46504	2416	3.24	0.981	30.05	0.2017	BE23712	KNSTD	24.49±0.41	106.4±1.8	3786	63	200
ARO-13	46.01694	7.46577	2398	2.26	0.974	30.32	0.2041	BE23713	KNSTD	21.05±0.35	91.6±1.5	3320	55	170
ARO-11	46.01675	7.46498	2419	3.79	0.981	20.80	0.1820	BE23711	KNSTD	15.78±0.39	89.0±2.2	3201	79	180
'LIA' COMPOSITE MORAINE, LIA SUB-RIDGE														
ARO-23	46.01815	7.4691	2308	2.84	0.948	47.03	0.1535	BE26085	07KNSTD	6.34±0.14	12.92±0.33	577	15	32
ARO-10	46.01598	7.46050	2475	1.83	0.988	30.48	0.2039	BE23710	KNSTD	3.27±0.11	13.71±0.48	475	16	28
ARO-9	46.01582	7.45993	2478	2.68	0.988	30.27	0.2037	BE23709	KNSTD	1.289±0.069	5.12±0.31	181	11	14
OUTER Post-LIA RECESSIONAL MORAINE														
ARO-66	46.01923	7.47315	2175	3.26	0.970	28.46	0.1558	BE32368	07KNSTD	0.998±0.058	3.55±0.22	170	10	13
ARO-63	46.0186	7.47057	2255	1.61	0.970	45.39	0.1553	BE32367	07KNSTD	1.470±0.064	3.30±0.15	148	7	10
ARO-67	46.01921	7.47357	2163	3.48	0.970	38.11	0.1563	BE32369	07KNSTD	1.145±0.067	3.06±0.19	148	9	12
ARO-65	46.01923	7.47315	2222	2.41	0.958	19.96	0.1846	BE31215	07KNSTD	0.453±0.029	2.38±0.20	111	9	11
ARO-64	46.01863	7.47058	2254	1.23	0.974	19.96	0.1842	BE31214	07KNSTD	0.447±0.031	2.33±0.21	104	10	11
INNER Post-LIA RECESSIONAL MORAINE														
ARO-62	46.01702	7.47225	2254	2.93	0.960	49.40	0.1248	BE32366	07KNSTD	1.532±0.072	2.53±0.12	116	6	8

Blank name	Processed with	Carrier (mg ^{9}Be)	Carrier (mg ^{9}Be)	$^{10}Be/^{9}Be$ Standard used	$^{10}Be/^{9}Be$ x10^{-14}	Total number of atoms ^{10}Be x 10^{3}
Blank_1_07Feb23	ARO-2,-3,-4,-5,-8	0.2035	BE23703	KNSTD	0.117±0.021	15.4±2.7
Blank_2_07Feb23	ARO-9,-10,-11,-12,-13	0.2051	BE23714	KNSTD	0.118±0.019	15.8±2.5
Blank_2_07Jan19	ARO-1,-6,-7	0.2065	BE23718	KNSTD	0.073±0.017	9.8±2.3
Blank_1_2010Jan22	ARO-15,-16,-18,-22	0.1895	BE28932	07KNSTD	0.116±0.021	14.3±2.5
Blank_3_08Oct06	ARO-23	0.1534	BE26086	07KNSTD	0.252±0.053	25.1±5.3
Blank_4_07Dec05	ARO-21	0.2066	BE24923	07KNSTD	0.747±0.013	10.0±1.8
Blank_1_2010Apr20	ARO-21 2010Apr	0.1868	BE29537	07KNSTD	0.150±0.023	18.7±2.8
Blank_2_2011Jan18	ARO-21_re,-52,-56,-59, -64,-65	0.1837	BE31218	07KNSTD	0.069±0.015	8.5±1.8
Blank_1_2011Jan18	ARO-55	0.1849	BE31221	07KNSTD	0.030±0.010	3.7±1.2
Blank_1_2011Oct4	ARO-62	0.1238	BE32567	07KNSTD	0.026±0.015	2.1±1.3
Blank_2_2011Oct4	ARO-63,-66,-67	0.1546	BE32376	07KNSTD	0.027±0.009	2.8±0.9

Table DR2: Radiocarbon dates on fossil soils within superimposed deposits of the LIA composite moraine (Figs. 1 and DR5A, DR5B) and detrital logs found in basal till of the proglacial streambed at Tsidjiore Nouve Glacier (Fig. DR5C) and glacier-climatic significance (Röthlisberger, 1976, Röthlisberger and Schneebeli, 1979). All calibrated ages below are given as 2σ intervals, referenced to the year 1950 CE (=BP, before present). They are calibrated with OxCal 4.1 (Bronk Ramsey, 2009, 2011) relative to the IntCal09 calibration data set (Reimer et al., 2009).

Dated material	Uncal. age (^{14}C-yr)	Cal. age (yr BP)	Glacier-climatic significance
Upper fossil soil in moraine	1075 ± 80	1180-800	Timing of 'favorable' (warm) climate, minimum age for moraine deposition
Lower fossil soil in moraine	1380 ± 85	1510-1080	
Fossil log	2940 ± 150	3440-2770	Timing of glacier advance, following a period of warmer climate
Fossil log	8400 ± 200	10120-8780	

Table DR3: Statistics of the ^{10}Be ages from the crest and the recessional ridges of the pre-LIA moraine including different mean ages with respective uncertainties and the reduced chi-squares. For the 'weighted mean', both mean age and uncertainty were weighted by the inverse variances (e.g. Taylor, 1997). The relative high chi-square value is a result of the exceptionally small 1σ analytical errors of the individual ages (~1.5%). Hence, for both crest and recessional ridges the boulder age distributions indicate that significant errors due to complex geological conditions (inheritance from prior exposure, erosion, or boulder instability) or snow cover are unlikely.

	^{10}B ages on crest (n = 10)	^{10}Be ages on recessional ridges (n = 7)
Arithmetic mean ± standard deviation	11,440 ± 380 years	11,230 ± 210 years
- incl. production rate uncertainty	11,440 ± 680 years	11,230 ± 590 years
Weighted mean	11,440 ± 60 years	11,250 ± 80 years
Peak age	11,470 years	11,190 years
Median age ± interquartile range	11,430 ± 730 years	11,230 ± 290 years
Reduced X^2	3.9	0.9

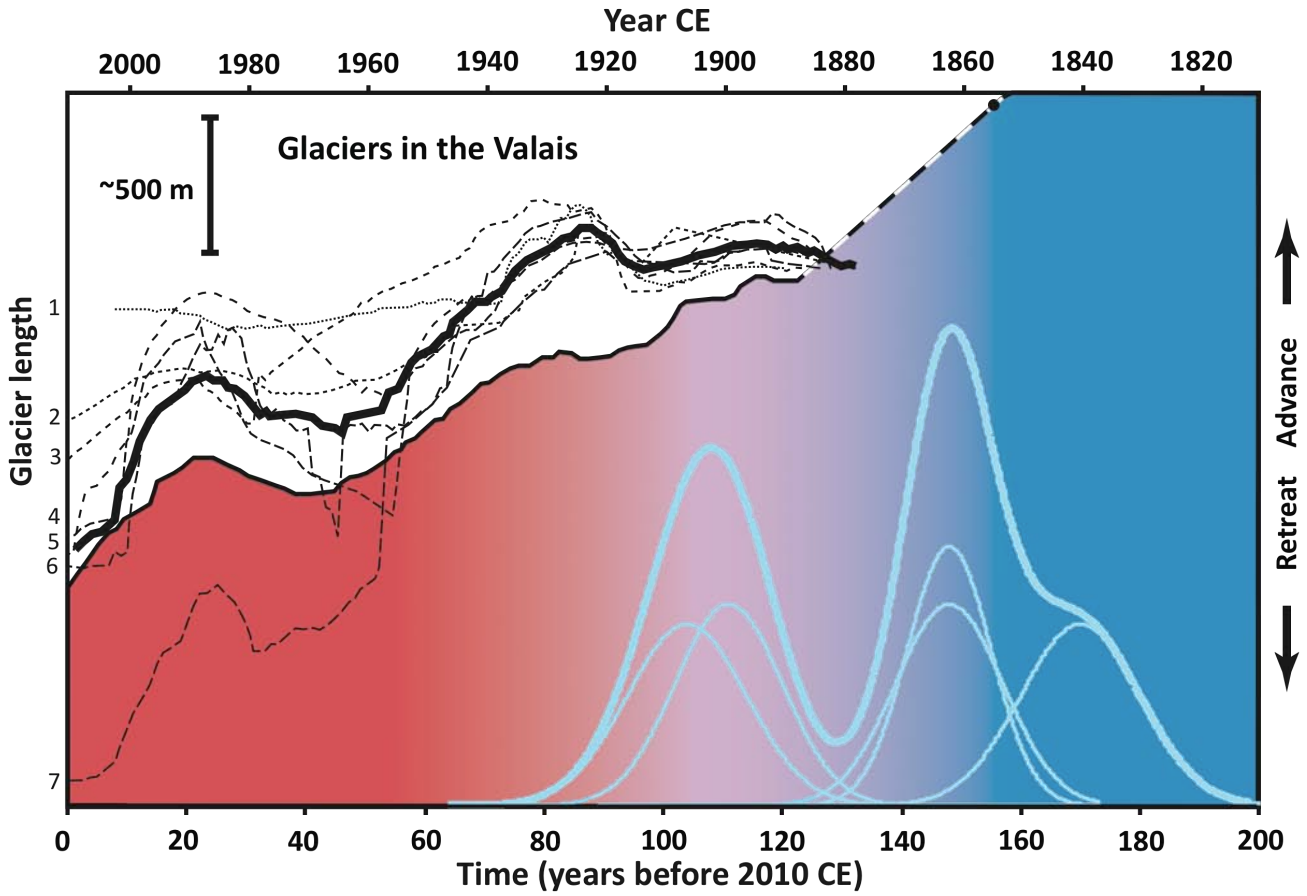

Fig. DR1: Post-LIA length measurements of several glaciers in the Valais, Switzerland. The red and dark blue graph shows length changes of Arolla Glacier (direct neighboring glacier of Tsidjiore Nouve; Glaciological reports, 1881-2009). The dashed thick line of this graph indicates lack of continuous measurements between the years 1856 and 1886. Thin superposed lines are length measurements of seven other glaciers in the Valais starting around the year 1880, with the thick black line representing their average: 1 Fee Glacier, 2 Schwarzberg Glacier, 3 Lang Glacier, 4 Rossbode Glacier, 5 Trient Glacier, 6 Allalin Glacier, 7 Findelen Glacier. All glaciers show similar fluctuation patterns, i.e. during the general retreat from the LIA maximum a two-fold re-advance occurred between 1890 and 1930 CE, followed by another re-advance between 1970 CE and 1990 CE. The thick light blue curve is the summed probability plot of the individual ^{10}Be ages (thin light blue curves) from the outer post-LIA moraine.

Fig. DR2: Examples of sampled boulders. A and B: ARO-1 (view west) and ARO-59 (view east), respectively, both embedded on the crest of the pre-LIA moraine. C: ARO-16, protruding from a recessional ridge of the pre-LIA moraine, view east.

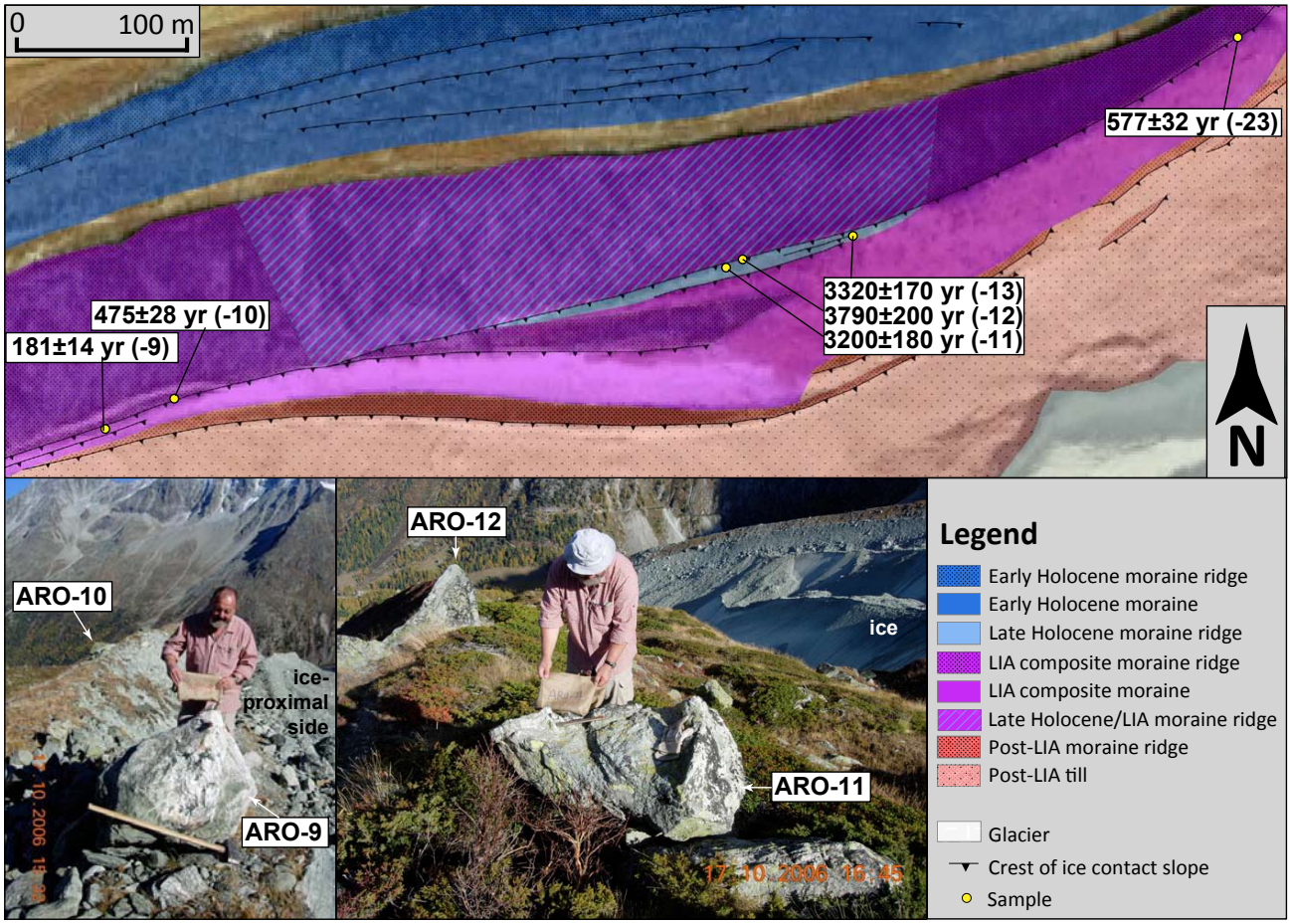

Fig. DR3: Positions of late Holocene and LIA boulders on the LIA composite moraine. The upper panel displays the corresponding sample sites and ages in a zoom-in of the moraine map given in Fig. 1. The left photograph shows the position of boulder ARO-9, which is on a more ice-proximal and thus stratigraphically younger subsection of the composite moraine than boulder ARO-10, in agreement with the ^{10}Be chronology. Similarly, the right picture shows that ARO-12 is in a slightly more ice-distal and therefore stratigraphically older position than ARO-11, again in agreement with the ^{10}Be ages.

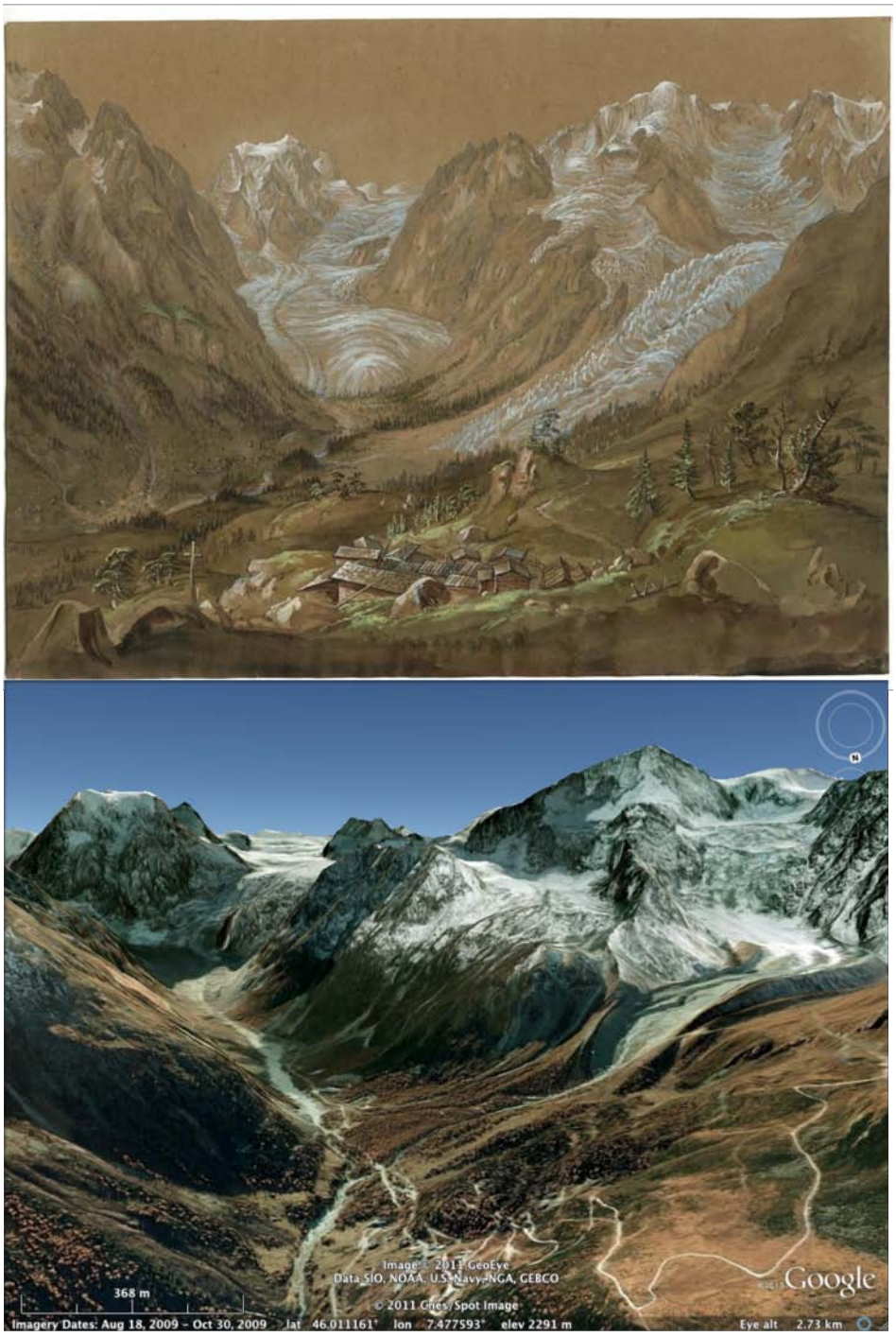

Fig. DR4: Upper panel: Drawing by Bühlmann from the year 1836 CE (Skizzenbücher Bd. 10, 256, Graphische Sammlung ETH, Zürich) showing the Tsidjiore Nouve Glacier on the right, the Arolla Glacier on the left and the village Arolla in the front. Glacier terminus positions are close to their Little Ice Age peak extent. Lower panel: Google Earth picture of approximately the same view in the year 2009 CE.

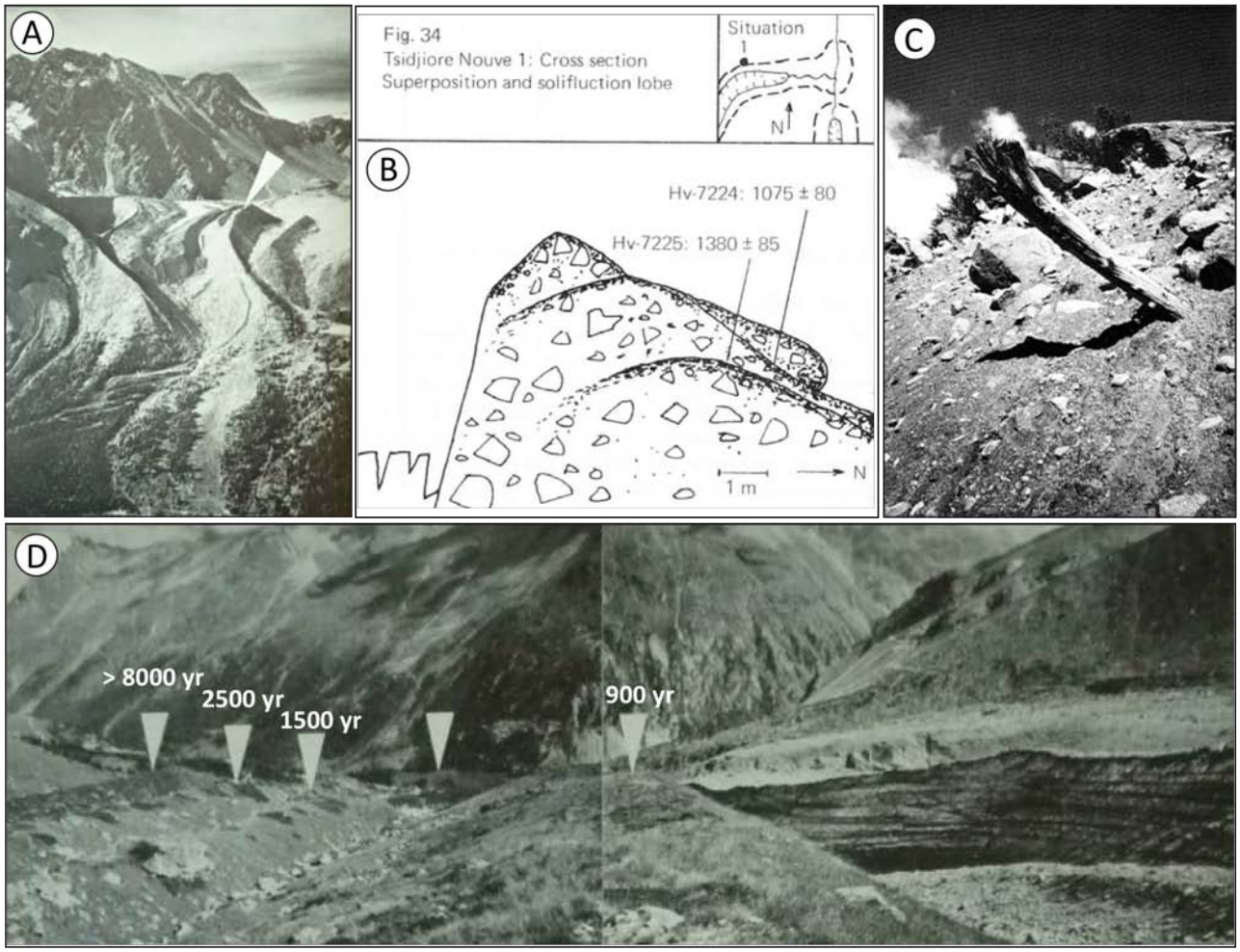

Fig. DR5: Figures from the earlier work on the Holocene moraine sequence at Tsidjiore Nouve Glacier (Röthlisberger, 1976; Röthlisberger and Schneebeli, 1979). A: Photograph of the glacier and the moraine sequence in the year 1972 with white arrow pointing to the location of the excavated fossil soils. B: Schematic illustration of the two fossil soils found in superimposed moraine deposits in the LIA composite moraine and corresponding ^{14}C ages. According to the authors, the younger fossil soil was covered by solifluction during a cold period. C: Radiocarbon dated larch log embedded in basal till and washed out by the glacial stream (3440-2770 cal years BP). D: Left lateral moraine sequence with pilot age estimates, which are based on 4 radiocarbon dates at Tsidjiore Nouve Glacier (summary in Table DR2) in combination with radiocarbon dates from the nearby glaciers Findelen, Mont Miné, and Ferpècle (Röthlisberger, 1976; Röthlisberger and Schneebeli, 1979). The deposition ages of 2500, 1500 and 900 years are presumably mostly inferred from ^{14}C ages at the three nearby glaciers. The white arrow in the back points to terminal moraine of the year 1817 CE.

References:

Balco, G., Stone, J., Lifton, N., and Dunai, T., 2008, A complete and easily accessible means of calculating surface exposure ages or erosion rates from 10Be and 26Al measurements, Quaternary Geochronology 3, p. 174-195.

Balco, G., Briner, J., Finkel, R. C., Rayburn, J. A., Ridge, J. C., and Schaefer, J. M., 2009, Regional beryllium-10 production rate calibration for late-glacial northeastern North America, Quaternary Geochronology 4, p. 93-107.

Bronk Ramsey, C., 2009, Bayesian analysis of radiocarbon dates, Radiocarbon, 51, p. 337-360.

Bronk Ramsey, C., 2011. OxCal Program 4.1, http://c14.arch.ox.ac.uk/oxcalhelp/hlp_contents.html

Glaciological reports (1881-2009) "The Swiss Glaciers", Yearbooks of the Cryospheric Commission of the Swiss Academy of Sciences (SCNAT) published since 1964 by the Labratory of Hydraulics, Hydrology and Glaciology (VAW) of ETH Zürich. No 1-126, (http://glaciology.ethz.ch/swiss-glaciers/).

Lal, D., 1991, Cosmic ray labeling of erosion surfaces: in situ nuclide production rates and erosion models, Earth and Planetary Science Letters 104, p. 424-439.

Reimer, P.J., and 27 others, 2009, IntCal09 and Marine09 radiocarbon age calibration curves, 0-50,000 years cal BP, Radiocarbon 51, p. 1111–1150.

Röthlisberger, F., 1976, Gletscher- und Klimaschwankungen im Raum Zermatt, Ferpècle und Arolla, Die Alpen 52, p.59-152.

Röthlisberger, F., and Schneebeli, W., 1979, Genesis of lateral moraine complexes, demonstrated by fossil soils and trunks: indicators of postglacial climatic fluctuations, *in* Schlüchter, C., ed., Moraines and Varves. A.A. Balkema, Rotterdam, p. 387-419.

Taylor J.R., 1997, An Introduction to Error Analysis. The Study of Uncertainties in Physical Measurements, University Science Books, Sausalito, 327 p.